Proceedings of the ASME 2021 40th International Conference on Ocean, Offshore and Arctic Engineering
OMAE2021
June 21-30, 2021, Virtual, Online

OMAE2021-62612

IMPACT OF VARIOUS NANOPARTICLES ON THE VISCOUS PROPERTIES OF WATER BASED DRILLING FLUIDS

Muhammad Awais Ashfaq Alvi
University of Stavanger, Stavanger, Norway

Mesfin Belayneh
University of Stavanger, Stavanger, Norway

Arild Saasen
University of Stavanger, Stavanger, Norway

Sulalit Bandyopadhyay
Norwegian University of Science and Technology, Trondheim, Norway

ABSTRACT

Properly designed drilling fluid is a key element in achieving safe and effective drilling operations. Rheological parameters of drilling fluid determine the equivalent circulation density, the pump pressure, and hole cleaning efficiency. Also, they have a significant role in predicting the stability of drilling fluid under static and low shear rates. The chemical composition of the drilling fluid controls the rheological parameters. Recently, studies have shown that a small concentration of nano-sized materials in the drilling fluid can substantially impact the rheological parameters of the drilling fluids.

In this study, various nanoparticles (NPs) with different shapes, sizes, and surface charges were used to investigate their impact on the viscous properties of water-based drilling fluid. Bentonite and KCl water-based drilling fluids were used as the base fluids. NPs such as Iron oxide, Silica (SiO_2), and multi-walled carbon nanotubes (MWCNT) were added to these base fluids. Also, surface functionalization of the NPs with polymer and functional groups such as -OH and -COOH groups was done to compare the effect of bare NPs with surface functionalized NPs. Hershel-Buckley model with dimensionless shear rates was used to calculate the low and high shear curvature exponents, surplus stress, and yield stress of the samples.

Results indicate that NPs alter drilling fluid's viscous properties based on their sizes, shapes, and surface charges. Moreover, the functionalization of NPs also modifies the properties based on the functional group attached to the NPs surface. This work shows that changing the size, shape, and surface charge of NPs has impact on viscous parameters, and NPs with different properties can fine-tune the fluid's viscous properties based on the requirement for drilling fluid.

Keywords: Water-based Drilling fluids, Nanoparticles, Yield stress

NOMENCLATURE

NPs:	Nanoparticles
XG:	Xanthan gum
MWCNT:	Multi-walled carbon nanotubes

1. INTRODUCTION

Water based drilling fluid is a formulation of various additives such as viscosity modifiers (bentonite clay, polymers) weighting agents (Barite), shale swelling inhibitors (salts, silicates) and materials to control fluid loss (polymers). Properly selected additives help to achieve drilling fluid's functions such as minimizing formation damage, lubricating and cooling the drill bit, and lifting the cutting from the bottom hole to the surface [1, 2]. Viscous properties of drilling fluids are significant in achieving various purposes during a drilling operation. These include predicting the stability of drilling fluids at a low shear rate, such as the gel-forming ability of drilling fluid, which controls the settling of barite. Moreover, the viscous properties of drilling fluids control the equivalent circulation density (ECD) and pump pressure during drilling operation [3].

Nanoparticles (NPs) are emerged as multifunctional drilling fluid additives due to their superior chemical and physical properties. Studies show the ability of NPs to alter the viscous properties of drilling fluids [2, 4-7]. Various NPs with different types, shapes, and sizes have been used to study the effect on the viscous properties of drilling fluids. These studies show that by changing the type, size, and shape of NPs, different results can be achieved. For instance, Vryzas et al. [2] added iron oxide NPs to the bentonite suspension. Results indicate that NPs increases the yield stress values of bentonite suspension. Surface coating of NPs still increases the yield stress values of the suspensions. However, silica NPs show the opposite trend as they reduce base fluid's yield stress values. Mahmoud et al [4] also observed the contrasting behavior of iron oxide and silica NPs on the yield stress of calcium bentonite drilling fluid. Moreover, other studies with silica NPs show that silica NPs in bentonite-based drilling fluids reduce the plastic viscosity and yield point of fluids [5, 6].

Anoop et al. [7] studied the effect of carbon nanotubes (CNTs) on bentonite-based drilling fluids. A low concentration of CNTs increases the viscosity of drilling fluids. However, increasing particle loading reduces the viscosity of fluids, especially at high temperatures. A study done by Fazelabdolabadi et al. [8] shows that functionalization of CNTs increased the shear stress values of water-based drilling fluids., specifically at higher shear rates. Also, CNTs able to increase yield point and lowers the plastic viscosity of the base fluid. Also, Ismail et al. [9] show that MWCNT and silica NPs increase the yield point of water-based drilling fluid. A low concentration of NPs reduces the plastic viscosity of base fluid. Gel strength results show opposite trends for MWCNT and silica NPs, as silica NPs reduce gel strength while MWCNT increases the gel strength of base fluids. However, most of these studies were with simple bentonite-based fluids, and in field-scale weighted drilling fluids are commonly used. Therefore, in the current work, the effect of various NPs in weighted bentonite-based fluids were studied. KCl-based fluids were also studied, owing to their extended use because of their shale inhibitive properties.

Surface modification of NPs is usually done to improve the stability of NPs in an aqueous solution and to incorporate functional groups on the NPs surface to provide better interaction of the NPs with other materials. Magnetic NPs have high surface energies, which cause aggregation of NPs as they try to minimize their surface energies. Coating or grafting NPs with organic (i.e., polymers and surfactants) and inorganic molecules such as silica stabilize the NPs and attach functional groups on their surface [10]. Silica NPs stability in an aqueous solution can also improve by surface modification with silanes [11] and dispersing NPs in surfactant. Moreover, to keep MWCNTs stable in water, chemical methods such as dispersing nanotubes in surfactants and introducing functional groups (i.e., COOH and -OH) on their surface using acid treatment are used [12]. Composite NPs are used in several studies to improve the performance of drilling fluids [13, 14, 15]. In this study, both uncoated and surface functionalized NPs are used to study the effect on bentonite-based and KCl-based drilling fluids.

2. MATERIALS AND METHODS

A local service company provided drilling fluid additives such as bentonite, barite, xanthan gum (XG). KCl salt and soda ash were purchased from VWR Chemicals (Oslo, Norway). Multi-walled carbon nanotubes (MWCNT, MWCNT-OH, and MWCNT-COOH) dispersions in anionic surfactant were purchased from US Research Nanomaterials, Inc (Houston, TX, USA). Silica NPs (Si NPs) in powder form were purchased from Sigma Aldrich (Oslo, Norway). Surface modification of Si NPs was done with silane to incorporate sodium sulphonate on the surface of NPs, based on published studies [11,16,17]. Si NPs and Si-C were dispersed in de-ionized water. The third type of silica NPs was purchased from NYACOL Nano Technologies, Inc. (Ashland, MA, USA). NYACOL silica NPs were received as a 30 wt% dispersion in de-ionized water, with proprietary coating on the surface of NPs to provide long-term stability. Terms Si, Si-C, and Si-N are used for silica, surface modified and NYACOL NPs, respectively thought the text. Synthesis and coating of iron oxide NPs with XG was done based on our previous work [18]. Terms Fe NPs and Fe-XG NPs are used for iron oxide and iron oxide coated with XG throughout the text. Iron oxide NPs coated with silica were obtained from NTNU and called as Fe-Si NPs throughout the text.

2.1 Drilling Fluid Mixing

Two types of drilling fluids were prepared, bentonite-based and KCl-based. NPs with concentrations of 0.0095 wt% and 0.019 wt% were added to these base fluids. However, in case of Fe NPs high concentration of 0.038 wt% was also used to see the effect of higher concentration. The mixing procedure of drilling fluid preparation is based on our previous work [18]. To prepare bentonite drilling fluid soda ash, XG, and bentonite were mixed for 5 min followed by additional 5 min mixing to dislodge any material adhered to the mixing container. Afterward, barite was mixed for 5 min and an additional 5 min to dislodge any adhering materials to achieve the uniform mixing of components. NPs based drilling fluid was prepared by treating the based fluid with different concentrations of NPs (0.0095 wt%-0.038 wt%) and again mixed for 5 mins to disperse NPs in the drilling fluid. Hamilton Beach mixer was used to mix the drilling fluids. A similar procedure was used to mix KCl-based fluids with bentonite is replaced with KCl salt. Table 1 and 2 shows the composition of drilling fluids.

TABLE 1: CHEMICAL COMPOSITION OF BENTONITE-BASED FLUID

Material	Base Fluid	Base Fluid + NPs
Water	350 ml	350 ml
Soda ash	4.8 g	4.8 g
XG	0.71 g	0.71 g
Bentonite	10.04 g	10.04 g

Barite	183 g	183 g
NPs in water	-	0.05, 0.1, 0.2 g

TABLE 2: CHEMICAL COMPOSITION OF KCL-BASED FLUIDS

Material	Base Fluid	Base Fluid + NPs
Water	350 ml	350 ml
Soda ash	0.75 g	0.75 g
XG	1.5 g	1.5 g
KCl	24.80 g	24.80 g
Barite	175 g	175 g
NPs in water	-	0.05, 0.1, 0.2 g

2.2 NPs and Drilling fluid Characterization

Scanning Electron Microscopy (SEM)

To attain the images of NPs, a Supra 35VP model scanning electron microscope (SEM, Zeiss, Oberkochen, Germany) was used. NPs samples were deposited on the carbon tape, and a coating of palladium was applied to avoid the charging of samples during analysis

Dynamic Light Scattering (DLS)

Size distribution and zeta potential of NPs dispersed in de-ionized water were measured using Zetasizer Nano-ZS instrument (Malvern, Worcestershire, UK). Measurements were performed at 25 ºC and 50 ºC for all the NPs samples.

Viscosity Measurements

A rotational viscometer, Fann 900 (FANN, Houston, TX 77032, USA), was used to measure the viscosity of the drilling fluids. The measurements were done at three different temperatures (22 ºC, 50 ºC, 80 ºC) under atmospheric pressure condition. Measurements were done at speeds of 600, 300, 200, 100, 60, 30, 6, and 3 revs/min.

2.3 Rheological Parameters of Drilling Fluids

In this work, the modified Herschel-Bulkley (H-B) model is used as H-B model is a relatively simple viscosity model giving good fit to viscosity measurements of drilling fluids for wide range of shear rates [3]. Herschel Bulkley model relates the shear stress, yield stress τ_y, shear rate $\dot{\gamma}$, flow index n and consistency index K by equation 1,

$$\tau = \tau_y + K(\dot{\gamma})^n \tag{1}$$

However, Saasen and Ytrehus [3] concluded that Herschel-Bulkley model does not always describe the drilling viscosity curve accurately for all shear rates. They show that the consistency index alone cannot provide information regarding the physical dependencies of the drilling fluid. Numerical values of the consistency index are dependent on the flow index as k=k(n). Therefore, it cannot be obtained directly from fluid measurement and should be estimated using algebraic operation. Moreover, different values of k and n provide similar flow curves. Therefore, modification of the Herschel Buckley model was done by Saasen and Ytrehus [3]. The model with the dimensionless shear rate is shown in equation 2,

$$\tau = \tau_y + \tau_s \left(\frac{\dot{\gamma}}{\dot{\gamma}_s}\right)^n \tag{2}$$

In equation 2, $\tau_s = \tau - \tau_y$ at $\dot{\gamma} = \dot{\gamma}_s$, where τ_s is a surplus shear stress, while $\dot{\gamma}_s$ is surplus shear rate. In this work, 170.3 1/s is used as surplus shear. Shear curvature exponent n at low and high shear is calculated using the following equation,

$$n = \frac{\ln\left(\frac{\tau_x - \tau_y}{\tau_s}\right)}{\ln\left(\frac{\dot{\gamma}_x}{\dot{\gamma}_s}\right)} \tag{3}$$

Shear stress (τ_x) measurements at shear rates ($\dot{\gamma}_x$) 51.11 1/s and 1022 1/s are used to calculate the numerical values of low shear curvature exponents (n_{ls}) and high shear curvature exponents (n_{hs}), respectively. Moreover, yield stress was calculated using $\tau_y = 2\tau_3 - \tau_6$, yield stress calculation following Zamora and Power [19] provide values with sufficient accuracy for hydraulic calculations [3].

In this paper, for the evaluation of the impact of NPs on the viscous properties of the bentonite and KCl-based drilling fluids, the modified Herschel Buckley model with dimensionless shear rate is used. It is important to mention here that the scope of the paper is limited to the evaluation of the effect of the NPs on the viscous parameters, and not to perform hydraulic calculations.

3. RESULTS AND DISCUSSION

3.1 Size Distribution and zeta potential of NPs

SEM images of the NPs are presented in Figure 1. MWCNT, MWCNT-OH, and MWCNT-COOH have 20-30 nm outside diameters and 5-10 nm inside diameters, with 10-30 µm lengths as provided by the manufacturer. Also, MWCNT-OH has 1.76 wt% -OH, and MWCNT-COOH has 1.23 wt% -COOH content. The size of the Si-NPs is in the range of 5-20 nm, while Si-N NPs have a particle size of 27 nm, as mentioned by the manufacturers. The size of the Fe NPs is around 11 nm, as reported in our previous study [18].

The hydrodynamic sizes and zeta potential values of NPs at 25 ºC and 50 ºC are shown in Tables 3 and 4. Surface functionalization of Fe NPs with XG and silica increases the sizes of NPs. Also surface modification of Si NPs increases the size, in case of Si-C NPs, as shown in Table 3. This shows the successful coating on the surface of NPs. The difference in the size of particles obtained from DLS and SEM is due to the difference in measurement principle as DLS measured the hydrodynamic radius of particles suspended in solution. In contrast, SEM measures the dry radius of the NPs as electrons transmitted through NPs sample. Also, DLS measurements are based on the assumption that particles are spherical. Therefore, the data for MWCNT may not be reasonable. However, the purpose of doing the measurement for MWCNT is to see the changes in size due to the functionalization of MWCNT with -OH and -COOH.

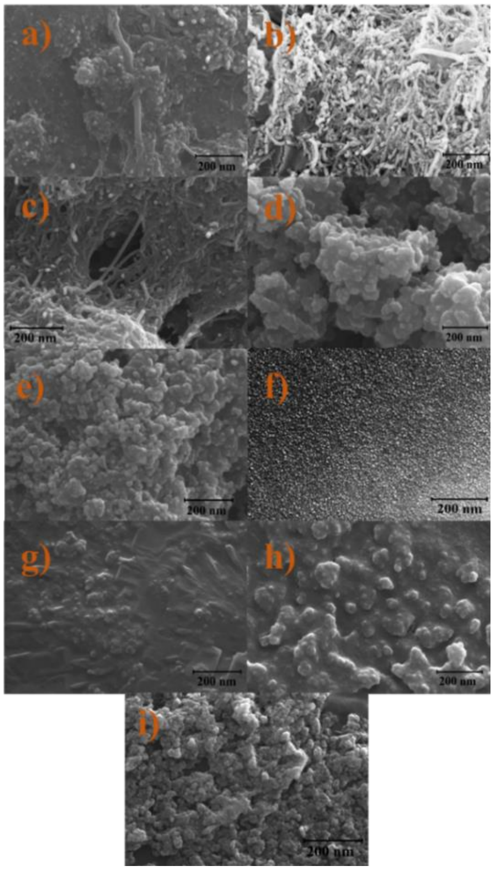

FIGURE 1: SEM IMAGES OF NANOPARTICLES a) MWCNT b) MWCNT-OH c) MWCNT-COOH d) Si-NPs e) Si-C f) Si-N NPs g) Fe NPs h) Fe-Si NPs i) Fe-XG NP

TABLE 3: SIZE AND ZETA POTENTIAL OF NPs AT 25 ºC

Nanoparticles	Size (nm)	Zeta Potential (mV)
MWCNT	161.8 ± 1.9	−26.2 ± 1.0
MWCNT-OH	158.1 ± 1.5	−30.1 ± 0.5
MWCNT-COOH	174.6 ± 2.7	−28.8 ± 0.4
Si NPs	217.3 ± 11.9	−36.1 ± 2.5
Si-C NPs	395.1 ± 29.4	−34.9 ± 2.2
Si-N NPs	36.8 ± 0.5	−35.8 ± 1.7
Fe NPs	273.5 ± 5.9	−31.3 ± 0.3
Fe-XG NPs	487.6 ± 8.6	−39.2 ± 0.6
Fe-Si NPs	634.7 ±102.5	−37.3 ± 1.4

Zeta potential measurements indicate that NPs used in this study have a negative surface charge. Size and zeta potential measurements at 50 ºC shows that NPs agglomerates at high temperature. Decrease in zeta potential dictate that NPs lose their stability at high temperature. However, results for MWCNTs, show that nanotubes are relatively stable at a higher temperature.

TABLE 4: SIZE AND ZETA POTENTIAL OF NPs AT 50 ºC

Nanoparticles	Size (nm)	Zeta Potential (mV)
MWCNT	189.8 ± 8.8	−27.5 ± 0.4
MWCNT-OH	216.2 ± 21.1	−29.3 ± 0.8
MWCNT-COOH	184.1 ± 12.7	−31.3 ± 0.5
Si NPs	676.8 ± 123.7	−15.4 ± 0.7
Si-C NPs	852.3 ± 161.2	−27.9 ± 1.2
Si-N NPs	46.1 ± 2.7	−26.5 ± 0.6
Fe NPs	381.2 ± 19.6	−20.8 ± 0.2
Fe-XG NPs	673.6 ± 65.5	−34.8 ± 0.4
Fe-Si NPs	1856.3 ± 161.2	−24.4 ± 0.4

3.2 Effect of MWCNTs on Rheological Parameters of Bentonite-Based Fluid

The bentonite-based fluids had a tendency to form strong gel at 80 ºC due to flocculation of clay platelets. For these fluids, because of the gel formation at lower shear rates, an increase in shear stress is measured while reducing the shear rate for some low shear rates at 80 ºC. Typical for these bentonite fluids the 5.11 1/s value is almost equal or slightly lower than the 10.22 1/s reading. For example, the base fluid shows shear stress of 15.30 Pa at 5.11 1/s and 15.33 Pa at 10.22 1/s. Therefore, there is increase in yield stress values and the flow indexes, n values become greater than unity, indicating shear thickening behavior. As mentioned before, the measurements shown in Figures 2 and 3, and later figures is to demonstrate the effect of the NPs. Therefore, use of the current parameters is still applicable. Moreover, a reduction in the flow index with addition of NPs is a sign of reduction of the gel strength formation.

The impact of MWCNT, MWCNT-OH, and MWCNT-COOH on n_{ls} and n_{hs} values for bentonite-based fluids is shown in Figure 2a-f. MWCNT shows most effect on n_{ls} at 80 ºC, as 0.0095 wt% and 0.019 wt% of nanotubes decreases the n_{ls} of base fluid by 51% and 84%, respectively as shown in Figure 2a. In case of MWCNT-OH, increasing the temperature to 80 ºC decreases the n_{ls} by 38% for 0.0095 wt% and 29% for 0.019 wt% of nanotubes. Moreover both 0.0095 wt% and 0.019 wt% MWCNT-OH increase n_{hs} values of base fluid, as shown in figure 2d. Figure 2 (e, f) shows the effect of MWCNT-COOH on n_{ls} and n_{hs} values of the base fluid. The addition of 0.0095 wt% of nanotubes decreases the n_{ls} by 26%, 16%, and 67% at 22 ºC, 50 ºC, and 80 ºC, respectively. MWCNT-COOH does not significantly affect the n_{hs} values of base fluid, as indicated in figure 2f.

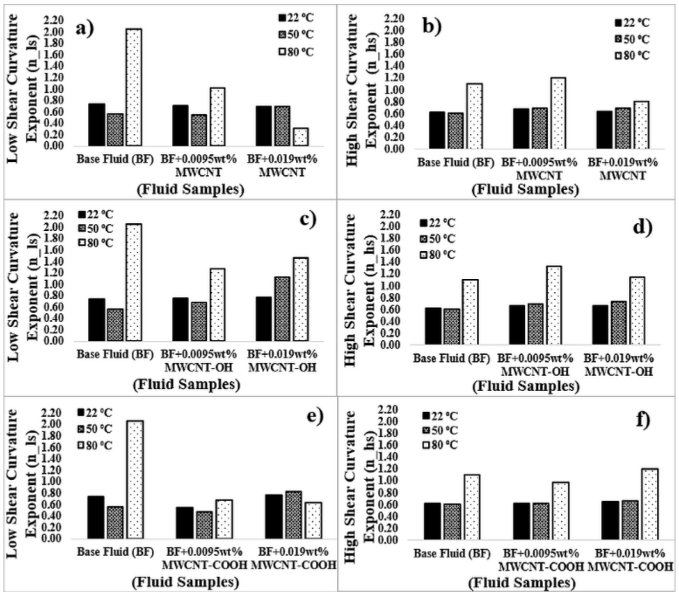

FIGURE 2: LOW AND HIGH SHEAR CURVATURE EXPONENT OF BENTONITE-BASED FLUIDS (a, b) MWCNT (c, d) MWCNT-OH (e, f) MWCNT-COOH (Please see Section 3.2 for general information about numerical values)

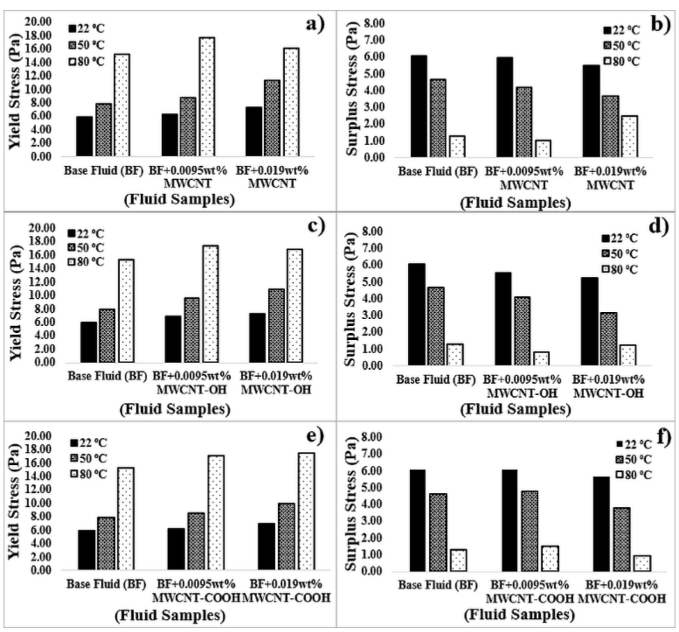

FIGURE 3: YIELD STRESS AND SURPLUS STRESS OF BENTONITE-BASED FLUIDS (a, b) MWCNT (c, d) MWCNT-OH (e, f) MWCNT-COOH

Figure 3 (a-f) shows yield stress and surplus stress values for bentonite-based fluids with MWCNTs. For 0.0095 wt% MWCNT, yield stress values are increased at all temperatures with 16% increment at 80 ºC. Further increase in concentration to 0.019 wt% also raises the yield stress, however at 80 ºC, there is only 5% increment in yield stress value compared to the base fluid as shown in figure 3a. Figure 3b shows that MWCNT decrease the surplus stress of base fluid by 22% at 80 ºC. However, for 0.019 wt%, at 80 ºC, the surplus stress is increased by 91% compared to the base fluid.

MWCNT-OH and MWCNT-COOH also increase the base fluid's yield stress values, as shown in Figures 3 (c-f). Figure 3c shows that 0.0095 wt% and 0.019 wt% MWCNT-OH increases the yield stress of base fluids. However, MWCNT-OH lowers the surplus stress values of the base fluid, for both 0.0095 wt% and 0.019 wt%, with the highest decrease of 36% at 80 ºC for 0.0095 wt% nanotubes in base fluid. For MWCNT-COOH, 0.019 wt% of nanotubes show more increment in yield stress values with 14% increase at 80 ºC. Like MWCNT-OH, surplus stress decreases for MWCNT-COOH at high particles concentration. In contrast, 0.0095 wt% nanotubes increase the surplus stress by 17% at 80 ºC.

MWCNT results show that nanotubes kept the n_{ls} and n_{hs} values of base fluid lower than 1 at high concentration. The surfactant acts as a dispersant and controls bentonite agglomeration at high temperatures. Anoop et al. [7] also show this behavior for nanotubes at higher concentrations. Moreover, yield stress results show that nanotubes able to interact with additives present in drilling fluid at low shear rates, with a higher concentration of MWCNT-OH and MWCNT-COOH increases yield stress at elevated temperature compared to MWCNT.

3.3 Effect of MWCNTs on Rheological Parameters of KCl-Based Fluid

Figure 4 (a-f) shows the n_{ls} and n_{hs} values of KCl-based fluids with MWCNT, MWCNT-OH, and MWCNT-COOH. Figure 4 (a, b) shows that an addition of 0.0095 wt% MWCNT slightly increases the base fluid's n_{ls} and n_{hs} values. An increase in the nanotube concentration forms two phases in the KCl-based fluids; due to high salt and surfactant concentration in the system, the fluids did not show any shear stress values at a lower shear rate. Therefore, values for n_{ls} and n_{hs} are not shown in Figure 4 (a, b). However, for MWCNT-OH and MWCNT-COOH, high concentration did not create two phases in the system, as shown in figure 4 (c-f). In case of 0.0095 wt% MWCNT-OH, there is minor increase in n_{ls} values as shown in figure 4c. However, for 0.019 wt% of nanotubes, n_{ls} decreased by 15% and 12% for 22 ºC and 50 ºC, respectively. Whereas, at 80 ºC, there is a slight increase of 5% in n_{ls} for base fluid with the addition of MWCNT-OH. Moreover, there is an increase in n_{hs} for both 0.0095 wt% and 0.019 wt% nanotubes at all temperatures, with the highest increase of 18% for 0.019 wt% at 80 ºC, as shown in Figure 4d. Addition of 0.0095 wt% and 0.019 wt% of MWCNT-COOH slightly increase n_{ls} values of base fluid at 80 ºC, as indicated in Figure 4e. Also, MWCNT-COOH increased the n_{hs} for both 0.0095 wt% and 0.019 wt% at all temperatures, except for a minor reduction at 50 ºC for 0.0095 wt% particles.

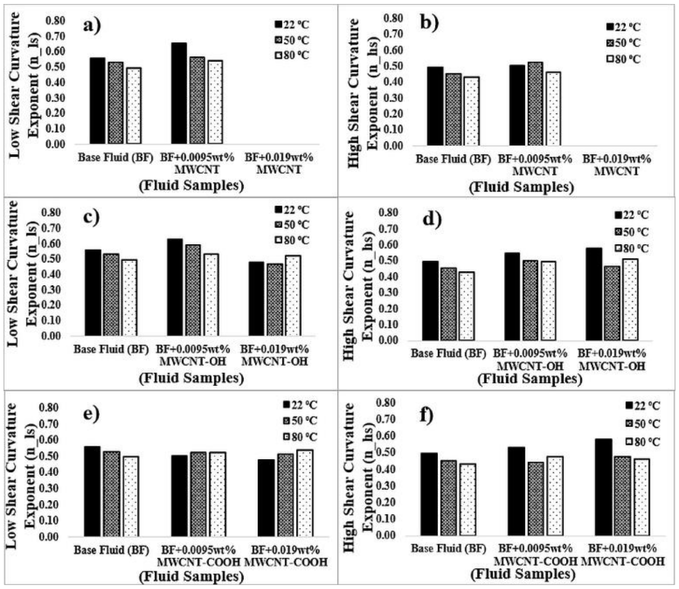

FIGURE 4: LOW AND HIGH SHEAR CURVATURE EXPONENT OF KCL-BASED FLUIDS (a, b) MWCNT (c, d) MWCNT-OH (e, f) MWCNT-COOH

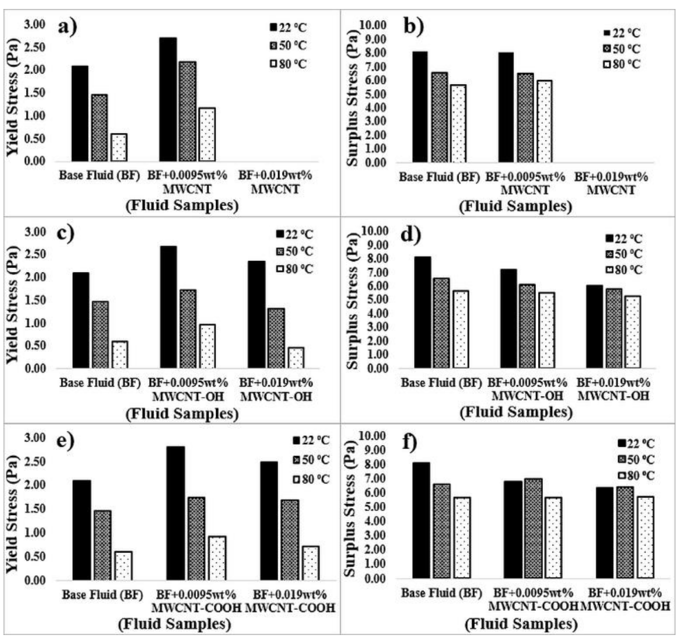

FIGURE 5: YIELD STRESS AND SURPLUS STRESS OF KCL-BASED FLUIDS (a, b) MWCNT (c, d) MWCNT-OH (e, f) MWCNT-COOH

The effect of MWCNT, MWCNT-OH, and MWCNT-COOH on yield and surplus stress of KCl-based fluids is presented in Figure 5. As shown in Figure 5a, there is a 95% increase in yield stress values for the 0.0095 wt% MWCNT at 80 ºC, respectively. However, at higher concentrations, i.e., 0.019 wt%, the absence of functional groups on nanotubes and high concentration of surfactant does not give any shear stress with applied shear strain. Surplus stress results presented in Figure 5b show that MWCNT has a minor effect and only offers a 5% increase for 0.0095 wt% at 80 ºC. In comparison, 0.0095 wt% of MWCNT-OH increases yield stress by 62 % at 80 ºC. Moreover 0.019 wt% shows slight reduction in yield stress values at 50 ºC and 80 ºC. Additionally, MWCNT-COOH, increases the yield stress of base fluid, with 53% increase at 80 ºC for 0.0095 wt%. Moreover MWCNT-OH and MWCNT-COOH have slight impact on surplus stress.

High concentration of MWCNT in the KCl-based system forms two phases in the fluid system due to aggregation & settling of barite and other additives. In case of MWCNT-OH and MWCNT-COOH, high particle loading still kept the drilling fluid system stable due to the presence of functional groups. Moreover, yield stress results show that MWCNT can increase yield stress, especially at high temperatures. This might be due to the interaction between nanotubes and xanthan gum.

3.4 Effect of Silica NPs on Rheological Parameters of Bentonite-Based Fluid

The effect of silica NPs on the bentonite-based fluids is presented in Figures 6 and 7. At 80 ºC, 0.0095 wt% of Si, Si-C, and Si-N NPs in base fluid decreases the n_{ls} by 44%, 42%, 45%, respectively. Increasing the concentration to 0.019 wt% further reduces the n_{ls} by almost 60% for all silica NPs. Similarly, NPs does not alter the n_{hs} of base fluids at 22 ºC and 50 ºC but do have a significant effect at 80 ºC, as shown in figure 6 (b, d, f). Si-NPs with 0.0095 wt% and 0.019 wt% concentration lowers n_{hs} of base fluid by almost 30%. Moreover, 0.0095 wt% & 0.019 wt% of Si-C and Si-N NPs in base fluid also show similar reducing trend in n_{hs} values.

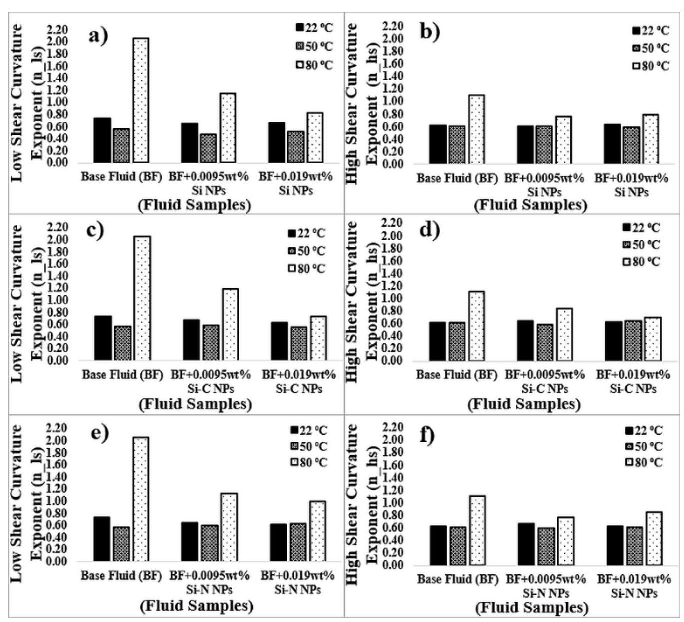

FIGURE 6: LOW AND HIGH SHEAR CURVATURE EXPONENT OF BENTONITE-BASED FLUIDS (a, b) Si NPs (c, d) Si-C NPs (e, f) Si-N NPs (Please see Section 3.2 for general information about numerical values)

Figure 7 (a-f) shows the impact of temperature and silica NPs on yield and surplus stress of bentonite-based fluids. Figure 7a shows that 0.0095 wt% of Si-NPs reduces the yield stress of base fluid by 48% at 80 ºC. An increase in NPs concentration to 0.019 wt% causes more reduction in yield stress and lowers the yield stress by almost 60% at all temperatures. Surface modified silica NPs, i.e., Si-C, also reduce yield stress of base fluid and achieve a reduction of 36% & 63% for 0.0095 wt% and 0.019 wt% NPs respectively at 80 ºC. Additionally 0.019 wt% of Si-N NPs provide a reduction of up to 31% at 80 ºC. Figure 7 (b, d, f) indicates that Si NPs, Si-C NPs, and Si-N NPs do not affect surplus stress values of base fluids at 22 ºC and 50 ºC for both concentrations.

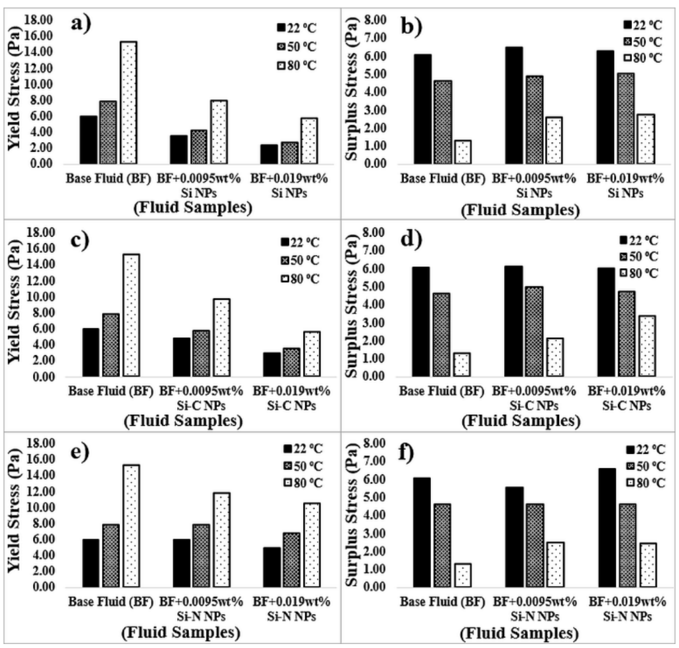

FIGURE 7: YIELD STRESS AND SURPLUS STRESS OF BENTONITE-BASED FLUIDS (a, b) Si NPs (c, d) Si-C NPs (e, f) Si-N NPs

NPs do increase the surplus stress values of base fluids at 80 ºC. As shown in figure 7 (b, d, f), NPs attain a 110% increase in surplus stress for 0.019 wt% Si NPs. Si-C NPs with the same concentration further increases the surplus stress of base fluid by 159%. However, 0.019 wt% of Si-N NPs shows a slightly less reduction of 87%. The results show that silica NPs also reduce the shear thickening behavior of base fluid at high temperatures by reducing n_{ls} and n_{hs} values. NPs neutralizes the positive charge on the bentonite platelets and reduce the agglomeration of clay particles by creating repulsion between bentonite surfaces [6]. Yield stress results depict that NPs can reduce the excessive gel formation of base fluids, especially at high temperatures, by forming comparatively weaker structures at low shear rates. Lower yield stress ultimately provides high surplus stress, especially at 80 ºC.

3.5 Effect of Silica NPs on Rheological Parameters of KCl-Based Fluid

Figure 8 (a-f) presents the n_{ls} and n_{hs} values of KCl-based fluids with Si, Si-C, and Si-N NPs. Silica NPs have slight effect on base fluid's n_{ls} and n_{hs} values. At 80 ºC, 0.019 wt% of Si NPs and Si-C NPs shows around 15% increment in n_{ls}. Moreover almost 10% increase in n_{hs} was achieved for both Si NPs and Si-C at 80 ºC.

Similar to MWCNTs, silica NPs also increase the yield stress values of KCl-based fluid, as shown in Figure 9 (a, c, e). 0.019 wt% of Si NPs in base fluid attain 87% increase in yield stress at 80 ºC. Moreover, Si-C NPs show an increasing trend at low concentration, however increase in NPs concentration only provides around 35% improvement in yield stress of base fluid at 50 ºC and 80 ºC. Yield stress of base fluid increased with addition of 0.0095 wt% Si-N NPs at all temperatures. However, a slight decrease of 7% in yield stress occurs at 80 ºC for 0.019 wt% Si-N NPs. The addition of Si, Si-C, and Si-N NPs to the base fluid does not significantly impact the surplus stress values, as shown in Figure 9 (b, d, f).

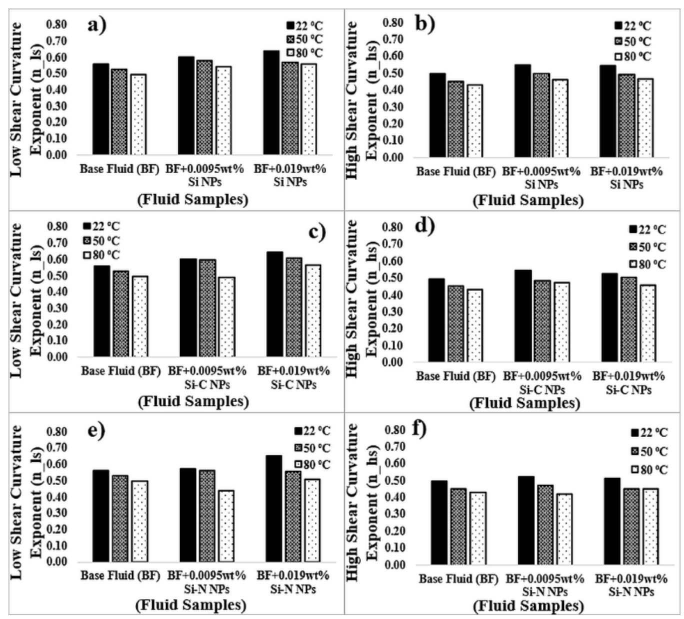

FIGURE 8: LOW AND HIGH SHEAR CURVATURE EXPONENT OF KCL-BASED FLUIDS (a, b) Si NPs (c, d) Si-C NPs (e, f) Si-N NPs

A high concentration of XG present in KCl-based fluids enables a slight increment in n_{ls} and n_{hs} values as polymer interacts with silane groups on silica NPs. Moreover, NPs increased the yield stress values of base fluid by keeping the drilling fluid stable at low shear stress. This increase in yield stress minimizes the available surplus stress.

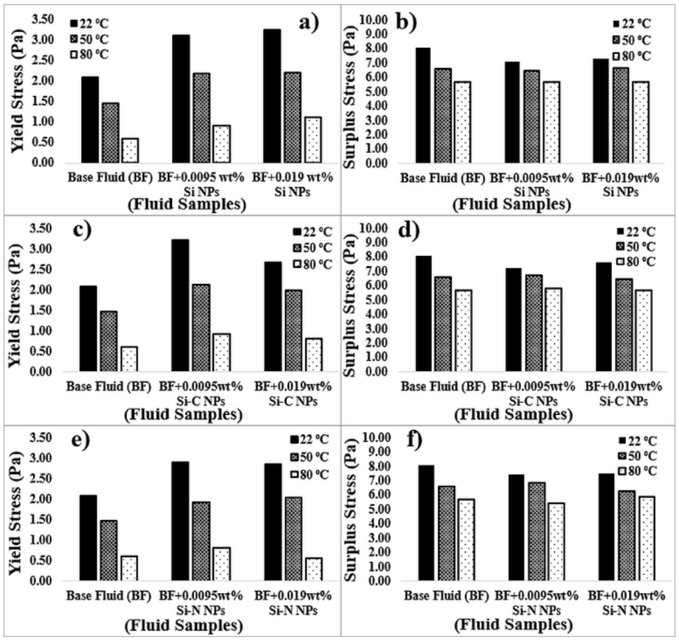

FIGURE 9: YIELD STRESS AND SURPLUS STRESS OF KCL-BASED FLUIDS (a, b) Si NPs (c, d) Si-C NPs (e, f) Si-N NPs

3.6 Effect of Iron oxide NPs on Rheological Parameters of Bentonite-Based Fluid

Impact of Fe NPs on n_{ls} and n_{hs} of base fluid is shown in Figure 10. As shown in figure NPs have significant impact on base fluid at higher temperature. For instance, Fe NPs decreases n_{ls} by 17% and increases n_{hs} by 80%, at 80 ºC for 0.0095 wt% concentration as shown in figure 10 (a, b). Additionally, 0.019 wt% of Fe NPs lowers the n_{ls} and n_{hs} by 54% and 7% at 80 ºC, see figure 10 (a, b). Raising the NPs concentration to 0.038 wt% increases the base fluid's n_{ls} and n_{hs} values, with the highest increase of 30% and 23% respectively at 80 ºC as indicated in figure 10 (c, d). Fe-XG NPs also increase the n_{ls} of base fluid by 30% and 35% at 50 ºC and 80 ºC, respectively. Although Fe-XG NPs show a slight reduction of 12% in n_{hs} at 80 ºC. Moreover, at 80 ºC, 0.0095 wt% Fe-Si NPs slightly lowers the n_{ls}, and 0.019 wt% causes a considerable reduction of 47% in n_{ls} of the base fluid. Also, 0.019 wt% NPs reduces the n_{hs} by 30%, see Figure 10f.

Figure 11 presents the yield and surplus stress of bentonite-based fluids with Fe NPs. A lower concentration of 0.0095 wt% and 0.019 wt% Fe NPs raises the yield stress values of base fluids. Almost 20% increment in yield stress values is shown by 0.0095 wt% Fe NPs at 22 ºC and 50 ºC, while at 80 ºC, yield stress increases by 13%, see figure 11a. Besides, a 0.019 wt% NPs also showed increase in yield stress at 50 ºC, but there is a 1% reduction in yield stress at 80 ºC. Similarly, 0.038 wt% of NPs raised yield stress values of base fluid by 27%, 28%, and 12% at 22 ºC, 50 ºC, and 80 ºC, respectively. However, coating of XG there is a decrease of 8% in yield stress values at 80 ºC as shown in figure 11c. Coating of silica on Fe NPs surface also increases the yield stress at 22 ºC and 50 ºC for 0.0095 wt% Fe-Si NPs, with minor reduction at 80 ºC. Increasing the concentration of Fe-Si NPs to 0.019 wt% shows the opposite effect and reduces yield stress at all temperatures. Most reduction of 46% is shown at 80 ºC, see figure 11e. 0.0095 wt% and 0.038 wt% Fe NPs decreases the surplus stress of base fluid at all temperature, with most reduction of 78% for 0.0095 wt% NPs and 41% reduction for 0.038 wt% at 80 ºC. However, Fe-XG and 0.019 wt% of NPs increases the surplus stress values at 80 ºC, and provide 21% and 58% increase, respectively. Addition of 0.019 wt% Fe-Si NPs to base fluid increases the surplus stress as a high concentration of NPs lowers the yield stress of base fluid.

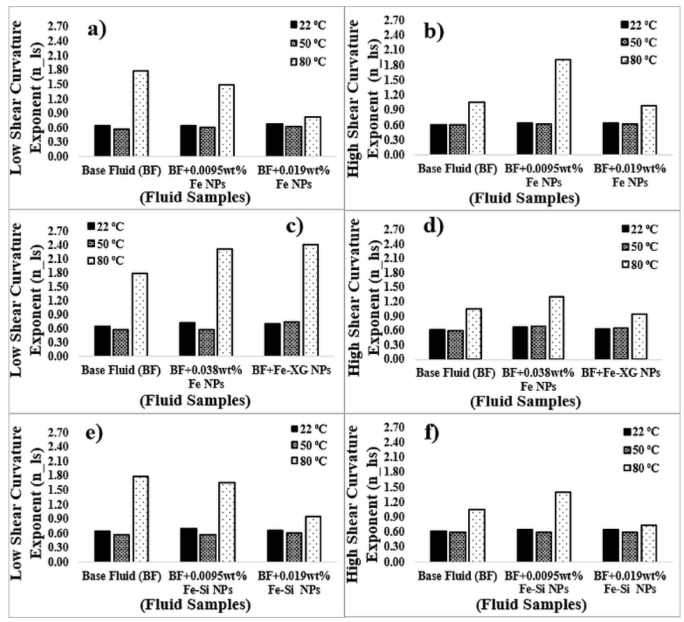

FIGURE 10: LOW AND HIGH SHEAR CURVATURE EXPONENT OF BENTONITE-BASED FLUIDS (a, b) Fe NPs (c, d) High conc and Fe-XG NPs (e, f) Fe-Si NPs (Please see Section 3.2 for general information about numerical values)

Results for bentonite-based fluids with Fe NPs show that at low concentration (0.0095 wt%), NPs slightly lowers the n_{ls}. However, 0.019 wt% further reduces the n_{ls} to less than 1 due to repulsion between the negatively charged NPs and clay platelets [18]. High n_{ls} values for 0.0095 wt% show that NPs adsorbed on clay platelets, which also increase the yield stress values of the base fluid. Although, 0.019 wt% creates slight repulsion between additives and reduces the yield stress at 80 ºC. Furthermore, a higher concentration of 0.038 wt% again increases the n_{ls}, n_{hs}, and yield stress values owing to an excessive agglomeration of magnetic NPs at this concentration [2]. Polymer coating improves the stability of NPs as indicated by zeta potential measurements. Still, n_{ls} show an increasing trend for Fe-XG, which suggests that NPs still tend to agglomerate. However, decreased n_{hs} and yield stress at 80 ºC shows that NPs provide some stability and control the agglomeration at high temperature and shear rate. Coating of silica NPs on the Fe NPs surface shows that silica presence reduces the n_{ls}, n_{hs}, and yield stress values of base fluids, precisely at 80 ºC for 0.019 wt% NPs. Moreover, due to yield stress reduction, there is a significant increase in surplus stress at 80 ºC for 0.019 wt% NPs.

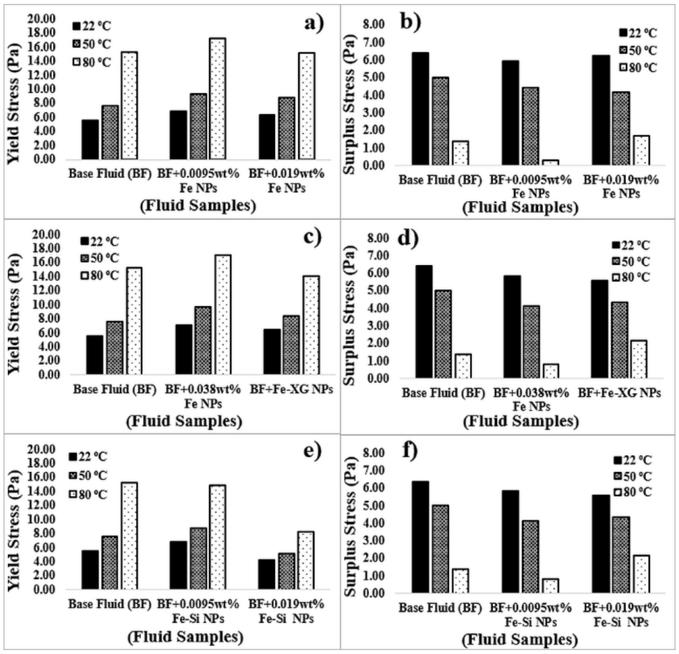

FIGURE 11: YIELD STRESS AND SURPLUS STRESS OF BENTONITE-BASED FLUIDS (a, b) Fe NPs (c, d) High conc. and Fe-XG NPs (e, f) Fe-Si NPs

3.7 Effect of Iron oxide NPs on Rheological Parameters of KCl -Based Fluid

Fe NPs with 0.0095 wt% and 0.019 wt% concentrations show a minor effect on n_{ls} and n_{hs} of KCl-based fluids, as shown in Figure 12 (a, b). Fe-XG NPs also have a slight effect on n_{ls} and n_{hs} of base fluids, with increasing n_{hs} by 10% at 80 ºC as shown in Figure 12d. For 0.038 wt% Fe NPs there is a 19% increase in n_{ls} of the base fluid, whereas a high concentration of NPs has a minor effect on n_{hs} of the base fluid. Fe-Si NPs also slightly impact the base fluid's n_{ls} and n_{hs} values, as shown in Figure 12 (e, f).

Figure 13 (a-f) shows the yield and surplus stress values of KCl-based fluids with Fe, Fe-XG, and Fe-Si NPs. Yield stress values of base fluid are increased for 0.0095 wt% and 0.019 wt% Fe NPs at 25 ºC and 50 ºC. However, at 80 ºC, there is a 10% reduction in yield stress of base fluid with the addition of 0.0095 wt% Fe NPs, while 0.019 wt% NPs still increase the yield stress by 6%. Increasing NPs concentration to 0.038 wt% shows a 63% increment in yield stress values at 22 ºC and 80 ºC, respectively.

Coating of polymer on Fe NPs (Fe-XG NPs) lowers the yield stress of base fluid at all temperatures, with a 15% reduction at 80 ºC. Moreover, 0.0095 wt% and 0.019 wt% of Fe-Si NPs increases base fluid's yield stress values. Addition of 0.019 wt% NPs to the base fluid increases the yield stress by 90% at 50 ºC and 56% at 80 ºC.

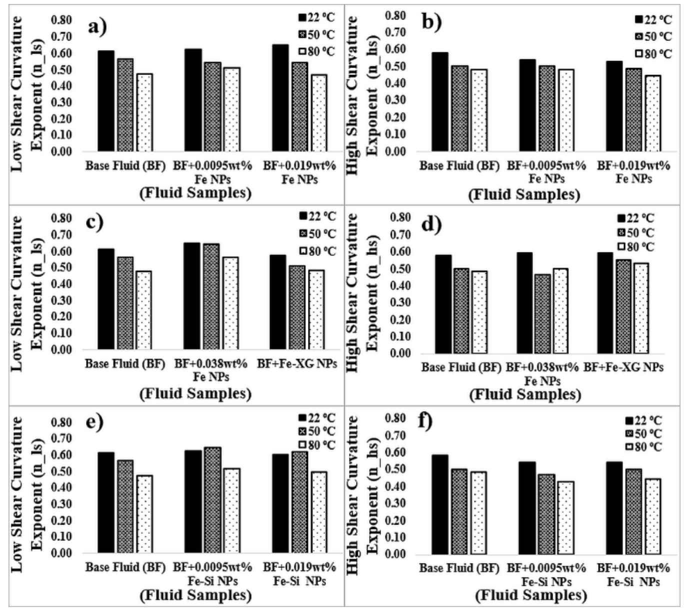

FIGURE 12: LOW AND HIGH SHEAR CURVATURE EXPONENT OF KCL-BASED FLUIDS (a, b) Fe NPs (c, d) High conc. and Fe-XG NPs (e, f) Fe-Si NPs

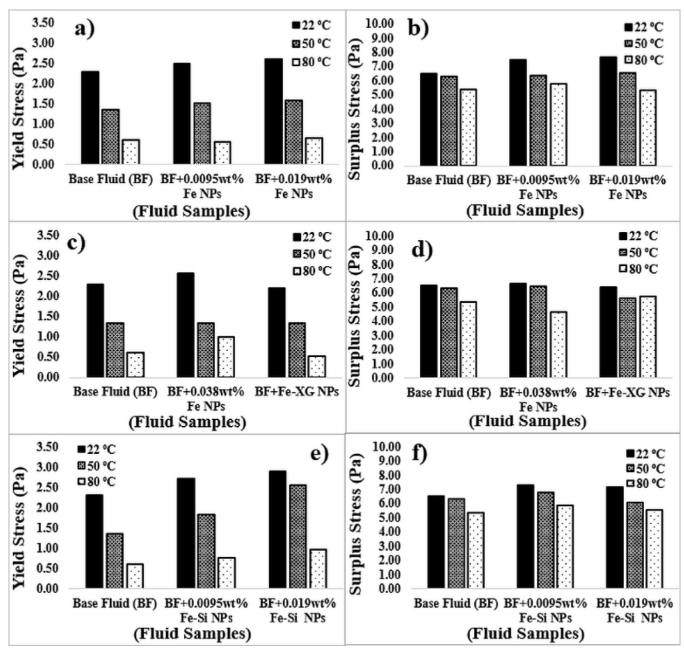

FIGURE 13: YIELD STRESS AND SURPLUS STRESS OF KCL-BASED FLUIDS (a, b) Fe NPs (c, d) High conc and Fe-XG NPs (e, f) Fe-Si NPs

Fe NPs shows a minor change in surplus stress of base fluid at high temperature. Higher concentration of NPs i.e. 0.038 wt% NPs decreases the surplus stress by 14% at 80 ºC. Moreover, Fe-XG shows a slight improvement in surplus stress of base fluid at 80 ºC. Fe-Si, NPs also have slight impact on surplus stress at all temperatures, as shown in figure 13 (e, f).

High salt concentration in KCl-based fluids reduces the stability of Fe NPs as NPs have a minor effect on n_{ls} and n_{hs}, yield stress values. However, agglomeration of NPs at 0.038 wt% concentration shows an increase in n_{ls}, n_{hs}, and yield stress at 80 ºC. Polymer coating on NPs again reduces the yield stress at 80 ºC due to the formation of weaker gel structures [20]. Furthermore, the presence of silica on the surface of NPs increases the yield stress at all temperatures due to better interaction of silica with xanthan gum and other drilling fluid additives.

4. CONCLUSION

The effect of MWCNT, silica, iron oxide NPs and Surface functionalized NPs on viscous properties of water-based bentonite and KCl drilling fluids has been studied. The main observations are summarized as follows:

In Bentonite-based fluids

- 0.019 wt% of MWCNT in base fluid kept the n_{ls} and n_{hs} values of the base fluid lower than 1 at 80 ºC. Moreover MWCNT-OH and MWCNT-COOH show more increase in yield stress at elevated temperature compared to MWCNT. Whereas MWCNT increase the surplus stress by 91% compared to the base fluid.
- Si, Si-C and Si-N NPs also reduce the shear thickening behavior of base fluid by reducing n_{ls} and n_{hs} values of base fluid at 80 ºC. Moreover 0.019 wt% of Si, Si-C and Si-N NPs in base fluid reduces the yield stress by 62%, 63% and 31% respectively at 80 ºC. While Si-C shows highest increase of 159% in surplus stress of base fluid.
- For iron oxide NPs, only 0.019 wt% of NPs kept the n_{ls} and n_{hs} values of base fluid less than 1. Yield stress values of base fluid is increases with 0.0095 wt% and 0.038 wt% NPs, while 0.019 wt% and Fe-XG slightly reduces the yield stress at 80 ºC. Fe-Si NPs reduces the n_{ls}, n_{hs}, and yield stress values of base fluids, precisely at 80 ºC for 0.019 wt% NPs.

In KCl-based fluids

- 0.0095 wt% of MWCNT, MWCNT-OH and MWCNT-COOH increases the yield stress of base fluid by 95%, 62% and 53% respectively at 80 ºC.
- In addition, Si, Si-C, Si-N slightly increases n_{ls} and n_{hs} of base fluid. Also, NPs increases the yield stress of base fluids.
- 0.038 wt% of Fe NPs in base fluid increases the n_{ls}, n_{hs}, and yield stress at 80 ºC. while, polymer coating on NPs (Fe-XG) again reduces the yield stress at 80 ºC due to the formation of weaker gel structures. Silica coating on NPs (Fe-Si NPs) increases the yield stress of base fluid.

The results are valid for the considered base fluids, NPs types, concentrations as well as the temperature and pressure conditions. Changing the conditions, one may achieve different results. However, from the results, it can be noted that NPs has significant impact on the conventional drilling fluids.

ACKNOWLEDGEMENTS

The first author acknowledges the Norwegian Ministry of Education and Research for financing the Ph.D. work. The Research Council of Norway is acknowledged for financial support to the Norwegian micro- and Nano-Fabrication facility, NorFab project number 245963. Also, authors thank Muhammad Bilal for providing help with DLS measurements.

REFERENCES

[1] Bourgoyne, AT, Millheim, KK, Chenevert, ME, & Young, FS (1986). Applied Drilling Engineering (SPE Textbook Series, Vol. 2). Society of Petroleum Engineers, Richardson, TX.
[2] Vryzas, Z., Nalbandian, L., Zaspalis, V. T., & Kelessidis, V. C. (2019). How different nanoparticles affect the rheological properties of aqueous Wyoming sodium bentonite suspensions. Journal of Petroleum Science and Engineering, 173, 941-954.
[3] Saasen, A., & Ytrehus, J. D. (2020). Viscosity models for drilling fluids—Herschel-bulkley parameters and their use. Energies, 13(20), 5271.
[4] Mahmoud, O., Nasr-El-Din, H. A., Vryzas, Z., & Kelessidis, V. C. (2018). Using ferric oxide and silica nanoparticles to develop modified calcium bentonite drilling fluids. SPE Drilling & Completion, 33(01), 12-26.
[5] Salih, A. H., & Bilgesu, H. (2017, April). Investigation of rheological and filtration properties of water-based drilling fluids using various anionic nanoparticles. In SPE Western regional meeting. Society of Petroleum Engineers.
[6] Katende, A., Boyou, N. V., Ismail, I., Chung, D. Z., Sagala, F., Hussein, N., & Ismail, M. S. (2019). Improving the performance of oil based mud and water based mud in a high temperature hole using Nanosilica nanoparticles. Colloids and surfaces a: physicochemical and engineering aspects, 577, 645-673.
[7] Anoop, K., Sadr, R., Yrac, R., & Amani, M. (2019). Rheology of a colloidal suspension of carbon nanotube particles in a water-based drilling fluid. Powder technology, 342, 585-593.
[8] Fazelabdolabadi, B., Khodadadi, A. A., & Sedaghatzadeh, M. (2015). Thermal and rheological properties improvement of drilling fluids using functionalized carbon nanotubes. Applied Nanoscience, 5(6), 651-659.
[9] Ismail, A. R., Aftab, A., Ibupoto, Z. H., & Zolkifile, N. (2016). The novel approach for the enhancement of rheological properties of water-based drilling fluids by using multi-walled carbon nanotube, nanosilica and glass beads. Journal of Petroleum Science and Engineering, 139, 264-275.
[10] de Dios, A. S., & Díaz-García, M. E. (2010). Multifunctional nanoparticles: analytical prospects. Analytica chimica acta, 666(1-2), 1-22.
[11] Weston, J. S., Jentoft, R. E., Grady, B. P., Resasco, D. E., & Harwell, J. H. (2015). Silica nanoparticle wettability: Characterization and effects on the emulsion properties. Industrial & Engineering Chemistry Research, 54(16), 4274-4284.

[12] Hilding, J., Grulke, E. A., George Zhang, Z., & Lockwood, F. (2003). Dispersion of carbon nanotubes in liquids. Journal of dispersion science and technology, 24(1), 1-41.
[13] Sadeghalvaad, M., & Sabbaghi, S. (2015). The effect of the TiO2/polyacrylamide nanocomposite on water-based drilling fluid properties. Powder Technology, 272, 113-119.
[14] Aftab, A., Ismail, A. R., Khokhar, S., & Ibupoto, Z. H. (2016). Novel zinc oxide nanoparticles deposited acrylamide composite used for enhancing the performance of water-based drilling fluids at elevated temperature conditions. Journal of Petroleum Science and Engineering, 146, 1142-1157.
[15] Jain, R., Mahto, V., & Sharma, V. P. (2015). Evaluation of polyacrylamide-grafted-polyethylene glycol/silica nanocomposite as potential additive in water based drilling mud for reactive shale formation. Journal of Natural Gas Science and Engineering, 26, 526-537.
[16] Margolese, D., Melero, J. A., Christiansen, S. C., Chmelka, B. F., & Stucky, G. D. (2000). Direct syntheses of ordered SBA-15 mesoporous silica containing sulfonic acid groups. Chemistry of Materials, 12(8), 2448-2459.
[17] Oh, Y. K., Hong, L. Y., Asthana, Y., & Kim, D. P. (2006). Synthesis of super-hydrophilic mesoporous silica via a sulfonation route. Journal of Industrial and Engineering Chemistry, 12(6), 911-917.
[18] Alvi, M. A. A., Belayneh, M., Bandyopadhyay, S., & Minde, M. W. (2020). Effect of Iron Oxide Nanoparticles on the Properties of Water-Based Drilling Fluids. Energies, 13(24), 6718.
[19] Zamora, M., & Power, D. (2002). Making a Case for AADE Hydraulics and the Unified Rheological Model. AADE-02-DFWM-HO-13 presented at AADE Technology Conference "Drilling & Completion Fluids and Waste Management", Houston, Texas, USA, 2-3 April.
[20] Chang, W. Z., & Leong, Y. K. (2014). Ageing and collapse of bentonite gels—effects of Li, Na, K and Cs ions. Rheologica Acta, 53(2), 109-122.

